

Electropolymerisable bipyridine ruthenium(II) complexes: synthesis, spectroscopic and electrochemical characterisation of 4-((2-thienyl) ethenyl)- and 4,4'-di((2-thienyl) ethenyl)-2,2'-bipyridine ruthenium complexes

Viviane Aranyos^a, Anders Hagfeldt^a, Helena Grennberg^b, Egbert Figgemeier^{a,*}

^a Department of Physical Chemistry, University of Uppsala, P.O. Box 579, Uppsala S-75123, Sweden

^b Department of Organic Chemistry, University of Uppsala, P.O. Box 599, Uppsala S-75124, Sweden

Received 16 July 2003; accepted 21 October 2003

Abstract

Four new ruthenium polypyridyl complexes with mono- or di-((2-thienyl) ethenyl) substituted bipyridines have been synthesized. The complexes were characterized by NMR, elemental analysis, UV–Vis absorption and electrochemistry (differential pulse and cyclic voltammetry). Electroactive polymer films of these complexes have been prepared by oxidative electropolymerisation and characterized by UV–Vis absorption spectroscopy and electrochemistry. The electrochemically induced polymerisation of the complexes resulted in a significant shift of the oxidation potential of the Ru(II)–Ru(III) process towards more positive potentials. Also, MLCT absorption band of the polymeric complexes is shifted towards shorter wavelengths. These results are interpreted in terms of an interruption of the conjugated system of the (2-thienyl)ethenyl-substituted bipyridine ligands due to a radical polymerisation mechanism affecting rather the ethenyl part of the ligand than the thienyl.

© 2003 Elsevier Ltd. All rights reserved.

Keywords: Electropolymerisation; Ru-complexes; Thiophene; Differential pulse voltammetry; 4-((2-Thienyl)-ethenyl)-2,2'-bipyridine; Redox-polymers

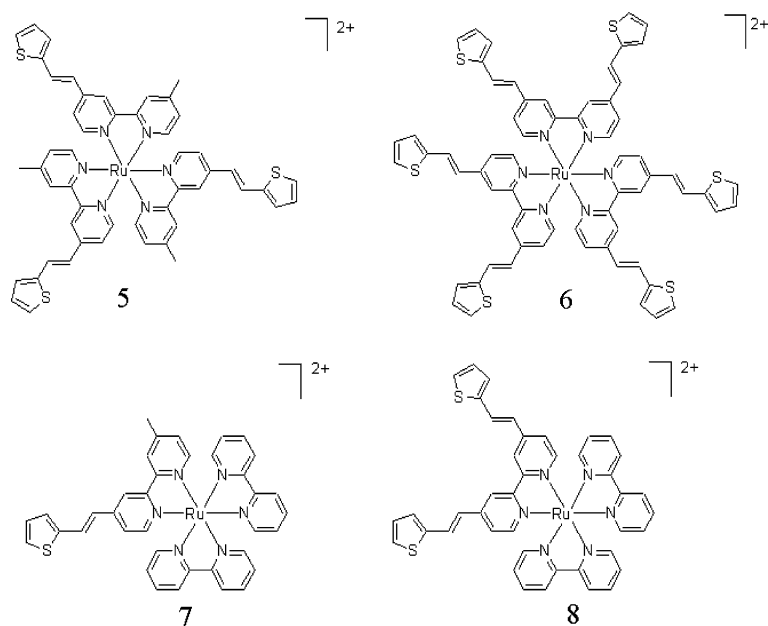
1. Introduction

Nano-structured dye-sensitized photoelectrochemical solar cells (NSCs) and solar cells based on conjugated polymers are considered as promising routes to decrease significantly the price of electricity by means of solar power in the future [1,2]. Moreover, these types of solar cells have features like flexibility and lightweight, which give them an even higher market potential. Nevertheless, polymer-based solar cells are currently using either Buckminsterfullerenes or polymers as electron acceptors which is costly or triggers stability problems. On the

other side, the highly efficient nano-structured solar cells based on TiO₂ as electron acceptor are incorporating liquid electrolytes for the transport of charge, which is problematic in terms of stability and production. With this background it can be very beneficial to combine the advantages of conducting polymers and nano-structured TiO₂ in the design of a solar cell. In this context we are currently investigating Ru-complexes, which can act as dye sensitizers in NSCs, which are modified with thiophene substituents on the bipyridine ligands. These thienyl groups are thought to be used as starting points for a covalent link between the dye and a solid electrolyte as, e.g., polythiophene. Also, an extension of the absorption spectrum together with an increased hydrophobicity improving stability of the NSC towards water penetration gives these substituents a bright future in the field of photoelectrochemical solar cells. However, in order to apply this type of dyes in a complex system such

* Corresponding author. Present address: Departement Chemie, Universität Basel, Spitalstrasse 51, Basel CH-4056, Switzerland. Tel.: +46-18-471-3661; Fax: +46-18-471-3654.

E-mail address: egbert.figgemeier@fki.uu.se (E. Figgemeier).



Scheme 1.

as the NSC, the study of models compounds **5–8** (Scheme 1) is a necessity.

In the past we have presented the synthesis and properties of ruthenium *tris*-bipyridyl complexes with methoxystyryl substituents and the characteristics of electrochemically produced polymers [3]. Following up this investigation, we here report the synthesis and the study of some ruthenium polypyridyl complexes with hydrophobic polymer precursors as ethylene-thiophene. Electroactive polymers of these complexes have been prepared by oxidative electropolymerisation. The resulting materials have been characterized with UV–Vis spectroscopy and by means of electrochemistry.

2. Experimental

2.1. Materials

All reagents were from commercial sources and were used without further purification. Solvents were HPLC grade and were used without further purification with the following exceptions: Tetrahydrofuran (THF) was distilled from sodium, diisopropylamine (DIPA) and triethylamine (Et_3N), which were distilled from CaH_2 . For electrochemical experiments, acetonitrile (Fluka, $\text{H}_2\text{O} \leq 0.001\%$) stored over molecular sieves was used. Butyl lithium (BuLi) was stored in a desiccator under nitrogen and used as fresh (no precipitate) 1.6 M solutions in hexane. Trifluoroacetic acid (TFA) and trifluoroacetic acid anhydride (TFAA) were stored at -18°C and used as received. Tetrabutylammonium hexafluorophosphate ($(\text{TBA})\text{PF}_6$) (Aldrich, 98%) was dried

under vacuum at 120°C for 48 h before performing electrochemistry. Syntheses were performed under a nitrogen atmosphere. Transparent conducting oxide electrodes of fluorine-doped tin oxide (FTO) on a 3-mm glass support (sheet resistance $8\ \Omega/\text{square}$) were purchased from Liffey–Owens–Ford. Elemental analyses were performed by the Analytische Laboratorien, Lindlar, Germany.

2.2. Physical characterisation

NMR spectra (^1H NMR at 400 MHz and ^{13}C NMR at 100 MHz) were recorded on a Varian Unity 400 spectrometer for CDCl_3 and CD_3COCD_3 solutions unless otherwise stated. The chloroform signals at 7.26 ppm (for ^1H) or 77.0 ppm (for ^{13}C) and the acetone signals at 2.04 ppm (for ^1H) or 29.8 ppm (for ^{13}C) were used as indirect reference to TMS.

UV–Vis absorption spectra were recorded using a Hewlett-Packard 8453 diode-array spectrophotometer and referenced against a solvent blank (CH_3CN). The fluorine-doped tin oxide (FTO) electrodes with polymer films deposited on the surface were positioned against the wall of a 1-cm quartz cuvette containing CH_3CN . The absorption of the FTO glass substrates was subtracted from the measured spectra of the compound.

Electrochemistry was performed using a CH Instruments Model 660. Electrochemical workstation and a conventional three electrode cell with a silver wire as pseudo-reference electrode. After the experiments ferrocene was added as an internal reference and all potentials given are quoted against the ferrocene–ferrocenium redox couple.

2.3. Synthesis

2.3.1. Ligands

2.3.1.1. 4-Methyl-4'-(2-hydroxy-2-(2-thienyl) ethyl)-2,2'-bipyridine (1). LDA was formed by mixing 1.54 mL BuLi (1.6 M in hexane) with 0.39 mL of DIPA in 10 mL THF at -60°C under N_2 . The mixture was then stirred at room temperature for 1/2 h. Thereafter, 4,4'-dimethyl-2,2'-bipyridine (0.50 g, 2.48×10^{-3} mol) dissolved in 15 mL THF was added through a double tipped needle after the temperature was cooled to -40°C . The black reaction mixture was then stirred at room temperature during 1 h. The aldehyde (0.25 mL, 2.72×10^{-3} mol) was diluted in 10 mL THF and added the same fashion to the reaction mixture to form a yellow precipitate. After stirring for 1 h, the reaction was stirred into water and extracted with dichloromethane. The organic phase was then washed with brine and dried over MgSO_4 . The dried solution was then concentrated. NMR of the crude product showed more than 85% of conversion compared to the aldehyde and complete conversion compared to the bipyridine. The crude product was used in the next step without further purification. ^1H NMR (400 MHz) (CDCl_3) δ 8.54 (1H, d, $J = 4.8$ Hz, aromatic pyridine), 8.50 (1H, $J = 4.8$ Hz, d, aromatic pyridine), 8.30 (1H, broad s, aromatic pyridine), 8.21 (1H, broad s, aromatic pyridine), 7.26 (1H, multiplet, thiophene), 7.13 (2H, multiplet, aromatic pyridine), 6.96 (2H, multiplet, thiophene), 5.29 (1H, dd, $J = 7.6$ Hz, $J = 6$ Hz, benzylic alcohol), 3.21 (1H, d, $J = 7.6$ Hz, benzylic), 3.21 (1H, d, $J = 6$ Hz, benzylic), 2.43 (3H, s).

2.3.1.2. 4,4'-(2-hydroxy-2-(2-thienyl) ethyl)-2,2'-bipyridine (2). LDA was formed by mixing 3.72 mL BuLi (1.6 M in hexane) with 0.83 mL of DIPA in 20 mL THF at -60°C under N_2 . The mixture was then stirred at room temperature for 1/2 h. Thereafter, 4,4'-dimethyl-2,2'-bipyridine (0.50 g, 2.48×10^{-3} mol) dissolved in 15 mL THF was added through a double-tipped needle after the temperature was cooled to -40°C . The black reaction mixture was then stirred at room temperature during 1 h. The aldehyde (0.52 mL, 5.96×10^{-3} mol) was diluted in 10 mL THF and added in the same fashion to the reaction mixture to form a yellow precipitate. After stirring for 1 h, the reaction was stirred into water and extracted with dichloromethane. The organic phase was then washed with saturated aq. NaCl and dried over MgSO_4 . The dried solution was then concentrated yielding 0.836 g (2.04×10^{-3} , 75%) of the product. ^1H NMR (400 MHz) (CDCl_3) δ 8.58 (2H, m, aromatic pyridine), 8.30 (2H, broad s, aromatic pyridine), 7.26 (2H, multiplet, thiophene), 7.15 (2H, multiplet, aromatic pyridine), 6.99 (4H, multiplet, thiophene), 5.29 (2H, m, benzylic alcohol), 3.21 (2H, m, benzylic).

2.3.1.3. 4-Methyl-4'-(2-(2-thiophene) ethenyl)-2,2'-bipyridine (3). 4-Methyl-4'-(2-hydroxy-2-(2-thienyl) ethyl)-2,2'-bipyridine (2.30 mmol) was dissolved in 10 mL of CH_2Cl_2 under nitrogen. As trifluoroacetic anhydride (TFA) (3.90 mL, 27.6 mmol) was added dropwise, the reaction mixture became orange. The mixture was stirred overnight and then concentrated to dryness, dissolved into EtOAc (50 mL), washed with water (2×50 mL), dried over MgSO_4 and concentrated to dryness. The product was afforded as yellow crystals in 96% yield (0.616 g, 2.21 mmol). ^1H NMR (400 MHz) (CDCl_3) δ 8.85 (1H, d, $J = 5.6$ Hz, aromatic pyridine), 8.78 (1H, $J = 5.2$ Hz, d, aromatic pyridine), 8.55 (1H, broad s, aromatic pyridine), 8.35 (1H, broad s, aromatic pyridine), 7.81 (1H, d, $J = 16$ Hz, alkene), 7.60 (1H, dd, $J = 5.6$ Hz, $J = 1.2$ Hz, pyridine), 7.52 (1H, d, $J = 5.2$ Hz, pyridine), 7.42 (1H, d, $J = 5.6$ Hz, thiophene), 7.33 (1H, d, $J = 3.6$ Hz, thiophene), 7.11 (1H, dd, $J = 3.6$ Hz, $J = 5.2$ Hz, thiophene), 6.93 (1H, d, $J = 16$ Hz, alkene), 2.63 (3H, s, Methyl). ^{13}C NMR, 154.7, 151.2, 148.3, 147.9, 146.2, 146.0, 140.6, 131.6, 131.7, 130.9, 128.5, 128.4, 127.3, 124.4, 122.7, 122.4, 119.6, 21.8.

2.3.1.4. 4,4'-(2-(2-thiophene) ethenyl)-2,2'-bipyridine (4). Crude **2** (2.04×10^{-3} mol) was dissolved in 15 mL of CH_2Cl_2 under nitrogen. As trifluoroacetic anhydride (TFAA) (3.90 mL , 27.6×10^{-3} mol) was added dropwise, the reaction mixture turned orange. The mixture was stirred overnight and then concentrated to dryness, dissolved into EtOAc (50 mL), washed with water (2×50 mL), dried over MgSO_4 and concentrated to dryness. The product was afforded as a yellow powder in 37% yield (0.281 g, 7.54×10^{-3} mol). ^1H NMR (400 MHz) (CDCl_3) δ 8.73 (1H, d, $J = 5.2$ Hz, aromatic pyridine), 8.65 (1H, broad s, aromatic pyridine), 7.70 (1H, d, $J = 16$ Hz, alkene), 7.41 (1H, d, $J = 4.8$ Hz, pyridine), 7.32 (1H, d, $J = 4.8$ Hz, thiophene), 7.24 (1H, m, thiophene), 7.06 (1H, dd, $J = 3.6$ Hz, $J = 4.8$ Hz, thiophene), 6.94 (1H, d, $J = 16$ Hz, alkene). ^{13}C NMR, 148.1, 141.5, 131.1, 129.7, 129.4, 129.0, 128.4, 127.4, 124.2, 122.3, 119.3.

2.3.2. Homoleptic complexes

2.3.2.1. Tris-(4-methyl-4'-(2-thienylethenyl)-2,2'-bipyridine) ruthenium dihexafluorophosphate (5). $\text{RuCl}_3 \cdot x\text{H}_2\text{O}$ (0.079 g, 0.38 mmol) and **L** (0.321 g, 1.15 mmol) were stirred at reflux in a 20 mL mixture of EtOH and H_2O (1:1), under nitrogen during 24 h. The solution turned dark red. NH_4PF_6 (1.24 g, 7.66 mmol) dissolved in water was added to the reaction mixture, after which a brown precipitate appeared. The precipitate was filtered off, washed with water and ether. The product was dried under reduced pressure during 24 h and was afforded in 24% yield (0.115 g, 0.095 mmol). *Anal. Calc.* for $\text{Ru}(\text{Bpy-Th}_1)_3(\text{PF}_6)_2 + 4\text{H}_2\text{O}$ (Mol Form.: $\text{C}_{51}\text{H}_{42}$

$\text{F}_{12}\text{N}_6\text{P}_2\text{RuS}_3 \cdot 4\text{H}_2\text{O}$): C, 47.19; H, 3.88; N, 6.47. Found: C, 46.82; H, 3.89; N, 5.85%.

2.3.2.2. *Tris-(4,4'-(2-thienylethenyl)-2,2'-bipyridine) ruthenium dihexafluorophosphate (6)*. $\text{RuCl}_3 \cdot x\text{H}_2\text{O}$ (0.079 g, 0.89 mmol) and **L** (0.100 g, 0.268 mmol) were stirred at reflux in a 20 mL mixture of EtOH and H_2O (1:1), under nitrogen during 24 h. The solution turned dark red. NH_4PF_6 (0.145 g, 0.89 mmol) dissolved in water was added to the reaction mixture, after which a brown precipitate appeared. The precipitate was filtered off, washed with water and ether. The product was dried under reduced pressure during 24 h and was afforded in 68% yield (0.092 g, 0.45 mmol). *Anal. Calc.* for $\text{Ru}(\text{Bpy-Th}_2)_3(\text{PF}_6)_2 + 5\text{H}_2\text{O}$ (Mol. Form.: $\text{C}_{66}\text{H}_{48}\text{F}_{12}\text{N}_6\text{P}_2\text{RuS}_6 \cdot 5\text{H}_2\text{O}$): C, 49.59; H, 3.66; N, 5.26; Found: C, 49.23; H, 3.83; N, 4.50%.

2.3.3. Heteroleptic complexes

2.3.3.1. *Bis-2,2'-bipyridyl ruthenium dichloride [4]*. $\text{RuCl}_3 \cdot x\text{H}_2\text{O}$ (0.200 g, 0.96 mmol), 2,2'-bipyridine (0.316 g, 2.02 mmol) and LiCl (0.173 g, 4.08 mmol) were stirred at reflux in 20 mL reagent grade DMF under argon for 8 h. After the reaction had cooled to room temperature, 100 mL of reagent grade acetone was added. The solution was then refrigerated overnight at 0 °C. Filtration gave a red violet solution and dark green crystals. Those were washed with water (3×15 mL) and with ether (3×15 mL). The product was then dried at room temperature under reduced pressure for 24 h. ^1H NMR (CDCl_3) δ 10.07 (d, $J = 5.6$ Hz, 2H, aromatic), 8.15 (d, $J = 8$ Hz, 2H, aromatic), 7.99 (d, $J = 8$ Hz, 2H, aromatic), 7.84 (t, $J = 8$ Hz, 2H, aromatic), 7.55 (m, 4H, aromatic), 7.46 (t, $J = 8$ Hz, 2H, aromatic), 6.87 (t, $J = 5.6$ Hz, 2H, aromatic). ^{13}C NMR, 160.4, 157.9, 153.9, 152.6, 134.5, 133.4, 125.5, 124.7, 121.9, 121.7.

2.3.3.2. *Bis-2,2'-bipyridyl-(4-methyl-4'-(2-thienylethenyl)-2,2'-bipyridine) ruthenium dihexafluorophosphate (7)*. *Bis-2,2'-bipyridyl ruthenium dichloride* (0.050 g, 0.10 mmol) and 4,4'-(2-thienylethenyl)-2,2'-bipyridine (0.027 g, 0.10 mmol) were stirred at reflux in a 20 mL mixture of EtOH and H_2O (1:1), under argon for 1 h. The solution turned red. NaPF_6 (0.250 g, ~ 20 eq) was added to the reaction mixture, which was stirred overnight (18 h), resulting in an orange precipitate. The precipitate was filtered and dried under reduced pressure during 24 h to give 0.043 g (0.044 mmol, 42% yield) of *bis-2,2'-bipyridyl-(4-methyl-4'-(2-thienylethenyl)-2,2'-bipyridine) ruthenium dihexafluorophosphate*. ^1H NMR (CD_3COCD_3) δ 8.95 (substituted bipyridine, d, $J = 1.2$ Hz, 1H), 8.81 (non-substituted bipyridine, d, $J = 7.2$ Hz, 4H), 8.76 (substituted bipyridine, s, 1H), 8.23–8.18 (non-substituted bipyridine, m, 4H), 8.16 (substituted bipyridine, d, $J = 0.8$ Hz, 1H), 8.15–8.04 (non-substi-

tuted bipyridine, m, 4H), 7.98 ($-\text{CH}=\text{CH}-$, d, $J = 16$ Hz, 1H), 7.91 (substituted bipyridine, d, $J = 6$ Hz, 1H), 7.86 (substituted bipyridine, d, $J = 5.4$ Hz, 1H), 7.64 (substituted bipyridine, dd, $J_1 = 6.4$ Hz, $J_2 = 2$ Hz, 1H), 7.62–7.55 (non-substituted bipyridine, m, 4H), 7.42 (substituted bipyridine, unresolved dd, 1H), 7.38 (substituted bipyridine, d, $J = 3.2$ Hz, 1H), 7.13 (substituted bipyridine, dd, $J_1 = 5.2$ Hz, $J_2 = 4$ Hz, 1H), 2.59 ($-\text{CH}_3$, s, 3H). *Anal. Calc.* for $\text{C}_{37}\text{H}_{30}\text{F}_{12}\text{N}_6\text{P}_2\text{RuS} \cdot 2\text{H}_2\text{O}$: C, 43.66; H, 3.37; N, 8.26; Found: C, 43.82; H, 3.21; N, 8.09%.

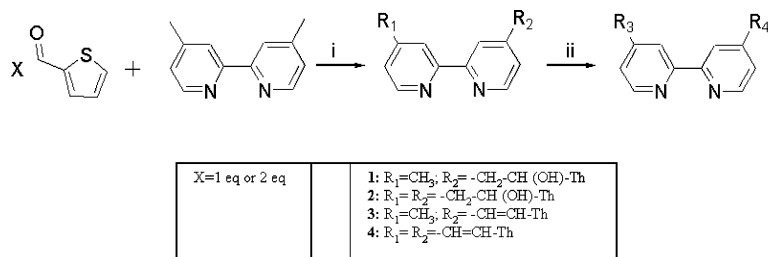
2.3.3.3. *Bis-2,2'-bipyridyl-(4,4'-(2-thienylethenyl)-2,2'-bipyridine) ruthenium dihexafluorophosphate (8)*. *Bis-2,2'-bipyridyl ruthenium dichloride* (0.050 g, 0.10 mmol) and 4,4'-(2-thienylethenyl)-2,2'-bipyridine (0.038 g, 0.10 mmol) were stirred at reflux in a 20 mL mixture of EtOH and H_2O (1:1), under argon for 1 h. The solution turned red. NaPF_6 (0.250 g, ~ 20 eq) was added to the reaction mixture, which was stirred overnight (18 h), resulting in an orange precipitate. The precipitate was filtered and dried under reduced pressure during 24 h to give 0.065 g (0.6 mmol, 60% yield) of *bis-2,2'-bipyridyl-(4,4'-(2-thienylethenyl)-2,2'-bipyridine) ruthenium dihexafluorophosphate*. ^1H NMR (CD_3COCD_3) δ 8.98 (substituted bipyridine, s, 2H), 8.81 (non-substituted bipyridine, d, $J = 8$ Hz, 4H), 8.21 (non-substituted bipyridine, t, $J = 8$ Hz, 4H), 8.16 (substituted bipyridine, d, $J = 5.6$ Hz, 2H), 8.05 (substituted bipyridine, d, $J = 5.2$ Hz, 2H), 7.97 ($-\text{CH}=\text{CH}-$, d, $J = 16$ Hz, 2H), 7.91 (substituted bipyridine, d, $J = 8$ Hz, 2H), 7.68 (dd, $J_1 = 6.4$ Hz, $J_2 = 2$ Hz, 2H), 7.62–7.55 (non-substituted bipyridine + substituted bipyridine, m, 4 + 2H), 7.40 (substituted bipyridine, broad d, $J = 3.8$ Hz, 2H), 7.68 (substituted bipyridine + $-\text{CH}=\text{CH}-$, dd + d, $J_1 = 5.2$ Hz, $J_2 = 3.8$ Hz, $J_3 = 16$ Hz, 4H). ^{13}C NMR, 157.7, 157.5, 152.0, 151.6, 146.8, 141.37, 138.2, 130.1, 129.8, 128.6, 128.1, 124.6, 124.1, 123.4, 122.6, 121.1. *Anal. Calc.* for $\text{C}_{42}\text{H}_{32}\text{F}_{12}\text{N}_6\text{P}_2\text{RuS}_2 \cdot 8\text{H}_2\text{O}$: C, 41.35; H, 3.97; N, 6.89; Found: C, 40.94; H, 3.41; N, 7.10%.

3. Results and discussion

3.1. Synthesis

A two-step synthesis was used to afford 4-methyl-4'-(2-(2-thiophene) ethenyl)-2,2'-bipyridine (ligand **3**), or 4,4'-(2-(2-thiophene) ethenyl)-2,2'-bipyridine (ligand **4**) as pictured in Scheme 2.

First, a nucleophilic addition of the mono- or di-anion of 4,4'-dimethyl-2,2'-bipyridine to 2-thiophenecarboxaldehyde (one or two equivalents) gave the corresponding alcohol (**1** or **2**) [4]. Dehydration was achieved using trifluoroacetic anhydride (TFAA) followed by precipitation. The preparation of the homo-



Scheme 2.

leptic complexes **5** and **6** was done in methoxyethanol (MeOEtOH) by mixing one equivalent of the ruthenium salt with three equivalents of the desired ligand (**1** or **2**). After the reaction mixture became dark red, the solution was cooled and the complex precipitated out of the solution by addition of (NH₄PF₆)-saturated water. The complex was filtered and dried under vacuum.

The heteroleptic complexes were prepared using a two-step synthesis. The dichloro bis-bipyridyl ruthenium complex was prepared according to a literature procedure [5]. The third ligand was introduced by mixing the dichloro bis-bipyridyl ruthenium salt to one equivalent of the mono- or di-substituted ligands followed by an exchange of the counter ion by addition of (NH₄PF₆)-saturated water.

3.2. Absorption properties

The absorption spectra for the ligands **2** and **4** were compared and clearly showed the substituent influence (see Fig. 1): ¹ The very typical Ligand Centered Charge Transfer (LCCT/ $\pi-\pi^*$) for bipyridine ligands is represented around 280 nm in both cases, and the conjugated thiophene gives an extra LCCT at \sim 340 nm [6].

The absorption properties of the different complexes have been recorded in acetonitrile and are shown in Fig. 2. ¹

The metal to ligand charge transfer (MLCT) correlates very well with the number of substituents on the molecules (see Table 1).

The more extended conjugated system is expected to have a smaller energy difference between its HOMO and its LUMO, which corresponds to a shift of the MLCT towards longer wavelengths.

The extinction coefficients reflect as well the structures of the complexes: The more extended conjugation on the complex leads to a shift of the MLCT towards longer wavelengths and a higher ϵ -value, although the variation between ϵ_{MLCT} for **7** and **8** is not significant, showing the little difference between the presence of one or two thiophene groups as substituents.

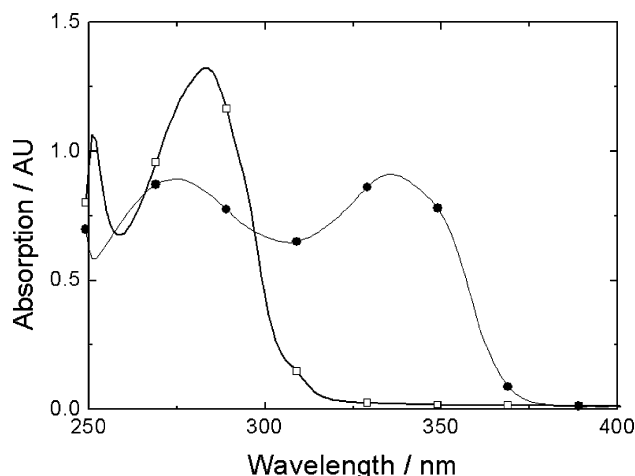


Fig. 1. Absorption spectra for both the conjugated and the non-conjugated thiophene substituted ligands **2** (-O-) and **4** (-●-) [7].

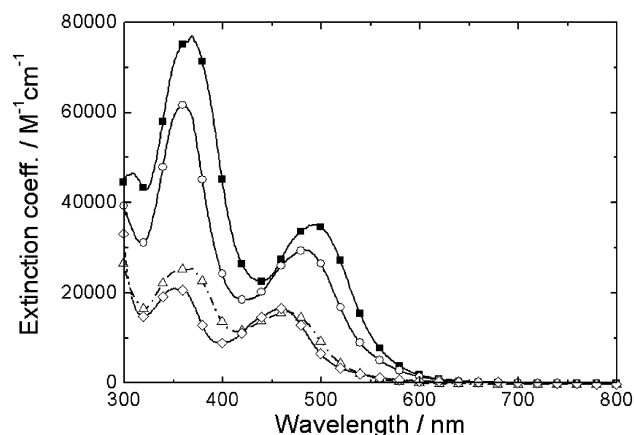


Fig. 2. Absorption spectra for the different complexes **5–8** (complex **5**: -O-; complex **6**: -■-; complex **7**: -◇-; complex **8**: -△-) (Footnote 1).

Table 1
Absorption properties of complexes **5–8** in acetonitrile

Complex	LCCT (nm)	ϵ_{LCCT}^a (mol ⁻¹ cm ⁻¹)	MLCT (nm)	ϵ_{MLCT}^a (mol ⁻¹ cm ⁻¹)
5	362	61 700	483	29 500
6	368	76 950	493	35 000
7	350	20 900	458	16 600
8	369 ^b	25 200	463	15 700

^a Extinction coefficient for the absorption maximum in the visible region.

^b The relatively high value is due to an artefact from the absorption spectrum. The average would be around 358.

¹ The symbols are for orientation purposes only and the spectra were measured with a 1 nm resolution.

Table 2
Electrochemical data for complexes **5–8** as determined by differential pulse voltammetry^{a,b}

Complex	Oxidation (V)	Reduction (V)
3	1.08	–1.24
4	1.08 (1.05)	–1.24
5	1.12 (0.98)	(0.75) 0.72
6	1.14 (1.21)	(0.74) 0.74
7	1.35 (1.20)	(0.90) 0.85
8	1.51 (0.90) 0.85	–1.62 –1.89 –2.12
[Ru(bpy) ₃] ²⁺	0.93	–1.69 –1.90 –2.14
[Ru(4,4'-dsty-bpy) ₃] ²⁺	0.83	
[Ru(Me2bpy) ₃] ²⁺	0.82	–1.75 –1.93 –2.17

^a In Volts. A glassy carbon electrode was used as working electrode, the redox couple Fc/Fc⁺ was used as internal reference and (TBA)₄PF₆ as electrolyte. The scan rate was 100 mV s^{–1}. The solvent was acetonitrile.

^b The values given in brackets are measured in dichloromethane

3.3. Electrochemical properties

The electrochemistry of complexes **5–8** was measured. All complexes were electrochemically active in CH₂Cl₂ and acetonitrile solution with 0.1 M (TBA)PF₆ as supporting electrolyte.² For comparison purposes also the ligands **3** and **4** were electrochemically investigated. The results are summarized in Table 2.

The redox potentials listed were measured by differential pulse voltammetry (DPV). A significant difference to numbers determined by cyclic voltammetry (CV) was not observed.

3.3.1. Oxidation

All complexes **5–8** showed in CV experiments at least one fully reversible peak in the oxidative region of the potential window, which can be assigned to the oxidation of Ru(II)–Ru(III). The position of the signal depends on the substitution of the bipyridine ligands. This oxidation characteristic is illustrated in Fig. 3.

As can be seen from Table 1, the Ru(II)–Ru(III) redox process of the homoleptic complexes **5** and **6** is shifted by slightly more than 100 mV towards less positive potentials in comparison to the heteroleptic complexes **7** and **8** and 200 mV relative to [Ru(bpy)₃]²⁺. This experimental result can be interpreted as a stabilisation of the Ru(III)-ion in these complexes relative to [Ru(bpy)₃]³⁺. Having two chemically very different substituents on the bpy-ligands (–CH₃ and –CH=CH–

² The complexes **5** and **6** showed only poor solubility in acetonitrile and dichloromethane (<0.5 × 10^{–4} mol/l), which is reflected in the low intensity of the electrochemistry shown in Fig. 3.

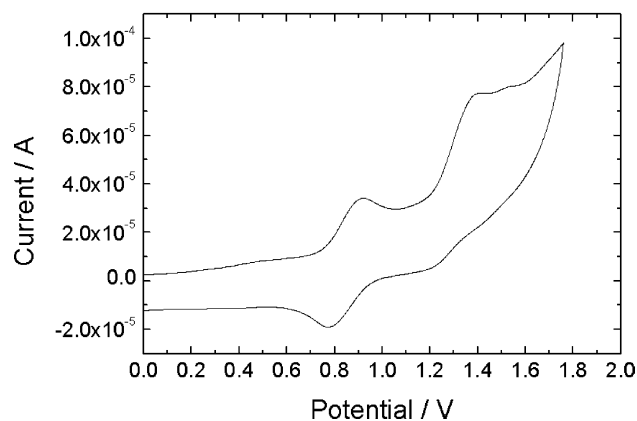


Fig. 3. Cyclic voltammogram of complex **7**. A glassy carbon electrode was used and the voltammogram was measured in acetonitrile with (TBA)PF₆ as supporting electrolyte at a scan speed of 0.1 V s^{–1}.

Th), the separation of the effects on the electronic structure within the complexes is difficult, but literature data of related compounds point out that both substituents are electron donating, which is stabilizing the oxidized state of the complex (Table 2) [7,8].

Beside the Ru(II)–(III) transition another – irreversible – oxidation process was observed for all complexes **5–8**. We assign these signals to a ligand-centred oxidation of the ethylene–thiophene substituent. A comparison with the electrochemistry of the uncoordinated ligand supports this assumption (see Table 2). Also in the literature, an oxidation of thiophene substituted polypyridine complexes was described at similar potentials [9,10].

Besides the influence of the different ligands on the oxidation potentials, an effect of the solvent was observed: Whereas the Ru(II)–Ru(III) transition remains at the same position when switching the solvent, the peaks assigned to the ethylene–thiophene oxidation were shifted by more than 100 mV to less positive potentials when changing the solvent from acetonitrile to CH₂Cl₂. To a smaller extent, such an effect was observed for thiophene oligomers for which the authors found a shift of 50 mV to less positive potentials when switching the solvent from acetonitrile to dichloromethane [11]. In the same contribution it was pointed out that the radical produced due to electrochemical oxidation is strongly stabilized by dichloromethane, which also was described generally before [12]. Therefore, we assign the shift of the second oxidation of the complexes to a solvent induced energetic stabilisation of the produced radical.

3.3.2. Reduction

Beside the electrochemical characteristics in the oxidative region of the potential window, the reduction of complexes **5–8** and the ligands **3** and **4** were investigated. The results are summarized in Table 2.

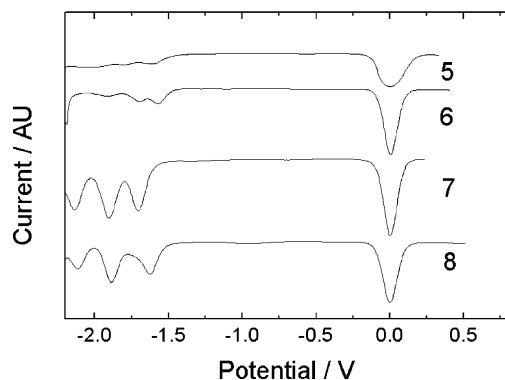


Fig. 4. DPV for compounds **5–8** (reductive region of the potential window). A glassy carbon electrode was used as working electrode, the redox couple Fc/Fc^+ was employed as internal reference and $(\text{TBA})\text{PF}_6$ (0.1 M in acetonitrile) as electrolyte.

For all complexes at least three signals were detected in CV and DPV (see Fig. 4) experiments at negative potentials within the potential window of acetonitrile and CH_2Cl_2 with $(\text{TBA})\text{PF}_6$ as the supporting electrolyte, which correspond to the successive reduction of the three bipyridine ligands [13].

As expected from this type of complexes, the difference in potential between the processes is close to 200 mV. A further reduction of the bpy-ligands was also observed as expected but not analysed³ [13].

Relative to the reduction potentials of $[\text{Ru}(\text{bpy})_3]^{2+}$, the values for the homoleptic complexes **5** and **6** are significantly shifted to less negative potentials for all three ligand centred processes. It can be assumed that the expansion of the conjugated system by the substitution of the bpy ligand with ethylene–thiophene groups is responsible for the lowering of the LUMO. On the other side, the methyl substituents seem to have a smaller or even opposite effect since the reductions of complex **5** are located at more negative potentials than for complex **6**. For the heteroleptic complex **7**, no significant shift of the reduction potentials relative to $[\text{Ru}(\text{bpy})_3]^{2+}$ were observed pointing out that methyl groups are rather lifting the LUMO level. This can be confirmed by a comparison with $[\text{Ru}(\text{bpyMe}_2)_3]^{2+}$ (Table 2). For complex **8**, we measured a less negative reduction process only for one ligand whereas the other two reductions are taking place at the same potentials as the equivalent processes in $[\text{Ru}(\text{bpy})_3]^{2+}$. This allows us to attribute the first reduction of complex **8** to a localisation on the ethylene–thiophene substituted bpy–ligand.

³ Differential pulse voltammetry had to be deployed for the determination of redox potentials since the cyclic voltammograms were dominated for the compounds **5**, **6** and **8** by polymerisation processes as discussed in the following section.

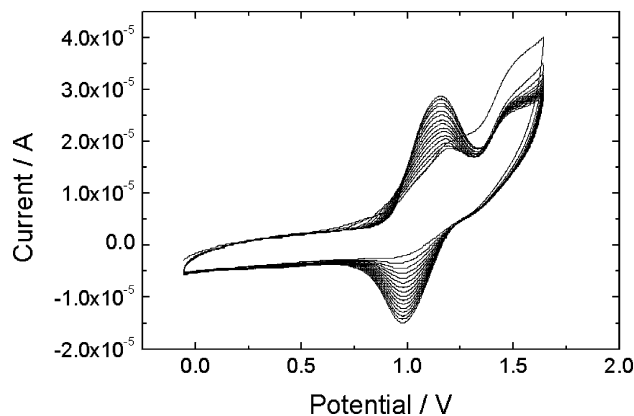


Fig. 5. Cyclic voltammogram for complex **6**. A glassy carbon electrode was used as working electrode, the redox couple Fc/Fc^+ was employed as internal reference and $(\text{TBA})\text{PF}_6$ (0.1 M in dichloromethane) as electrolyte at a scan rate of 100 mV s^{-1} .

3.3.3. Electrochemical polymerisation at positive potentials

For complexes **5**, **6** and **8**, an increase in intensity of the oxidation waves in the CV experiments were observed from one cycle to the next (see Fig. 5): The first scan gives an oxidation wave for the ruthenium center as well as a strong oxidation corresponding to the irreversible oxidation of the thiophene groups [14].

The oxidation waves merge together after the first scan in combination with a substantial growth of the peaks. One can also see a red–orange film deposited on the working electrode after the experiment. These effects were only seen when the potential window of the voltammetry experiments reached the oxidation of the complexes associated with the oxidation of the ethylene–thiophene ligand substituents. We assign these observations to a radical induced polymerisation as other authors described it for similar complexes leading to three-dimensional networks with the Ru in the backbone [15–21]. This polymerisation process was mainly observed in dichloromethane, whereas a stable effect in acetonitrile could only be seen for complex **6**. As discussed earlier, a stabilisation of radical cations was observed in dichloromethane relative to acetonitrile. It seems likely that besides the shift of the oxidation potential, the stabilisation of radicals favours a successful polymerisation, since the longer lifetime increases the probability of finding a thiophene counterpart for polymerisation. Also, the shift of the ligand centred oxidation towards less positive potential in dichloromethane increased the accessibility of the process within the potential window, decreasing the interferences with traces of water or solvent related processes. A typical example for the electrochemically induced polymerisation is given in Fig. 5 for complex **6**.

By cyclic voltammetry and DPV, one can see a tremendous shift (over 100 mV) of the oxidation potential of the $\text{Ru}(\text{II})$ – $\text{Ru}(\text{III})$ redox wave, indicating a change of

Table 3
Absorption and electrochemical properties of the complexes **5–8** (non-polymerized and oxidatively polymerized on FTO-glass support)

Complex	λ_{max} , MLCT (nm)		E_0 (V) (vs. Fc/Fc ⁺) ^a	
	Monomer	Polymer	Monomer	Polymer
5	483	472	0.72	0.85
6	493	475	0.74	1.07
7	485		0.85	
8	463	450		1.02

^a E_0 was determined in dichloromethane. The electrodes modified with a polymer were removed from the complex solution after polymerisation, rinsed with dichloromethane and then measured in dichloromethane/(TBA)PF₆ without the corresponding complex.

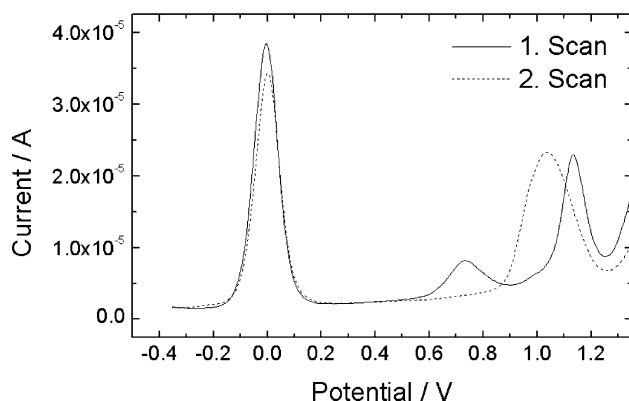


Fig. 6. DPV for complex **6**. A glassy carbon electrode was used as working electrode, the redox couple Fc/Fc⁺ was used as internal reference and (TBA)PF₆ (0.1 M in acetonitrile) as electrolyte. First scan – solid line and second scan – - - - dashed line.

the ligand's substituents polarity (see also Table 3). This effect can be seen most clearly for the polymerisation of complex **6** in acetonitrile.⁴ In Fig. 6 two successive DPVs are shown: The first scan shows two distinct peaks for the Ru(II)–Ru(III) and the ligand centred process, whereas the second scan only shows one strong peak – presumably the oxidation of the polymeric material on the electrode surface.

As discussed previously, the low oxidation potentials of complexes **5–8** relative to [Ru(bpy)₃]²⁺ has its origin in the increased size of the conjugated system of the bpy-ligand, therefore the strong shift of the oxidation potential is indicative of a loss of this conjugation. At the same time, the disappearance of the strong oxidation peak at 1.42 V is indicative of either a consumption or a cut of the thiophene groups from the conjugated system moving the oxidation potential of the group outside the potential window due to the polymerisation.

⁴ The same effect was also observed for complexes **5**, **6** and **8** in dichloromethane, but due to the close vicinity of the ligand and metal centred oxidations, the shift of oxidation due to polymerisation is less obvious than for the electrochemistry of **6** in acetonitrile.

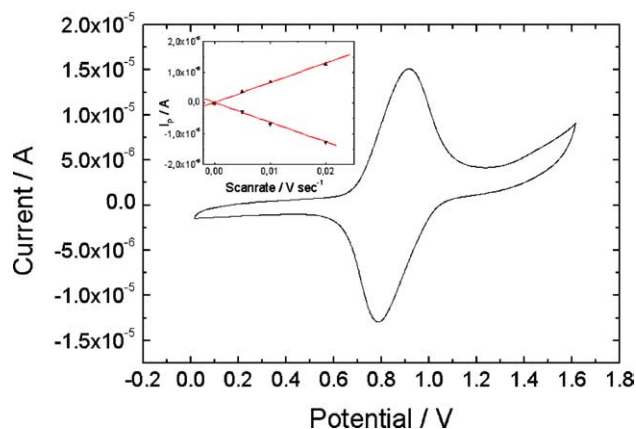


Fig. 7. Cyclic voltammogram of the polymer of complex **5** in CH₂Cl₂ with (TBA)PF₆ as supporting electrolyte and scan rate dependency of the peak current (inset).

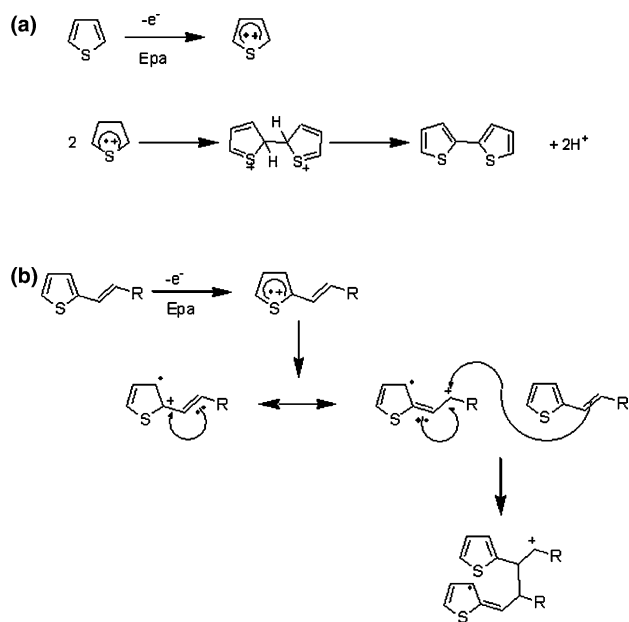
The electrochemistry of the polymers was also measured in monomer-free electrolyte. A typical cyclic voltammogram is presented in Fig. 7, and the values for the oxidation potentials are given in Table 3.

In all cases we find only one oxidation peak, which we relate to the Ru(II)–Ru(III) redox couple, whereas no further ligand-located oxidation as for the monomer was detected within the potential window. For a surface bound species, the separation between the oxidation and reduction peak is even at moderate scan rates rather high for a surface bound species. For the given example it is 130 mV at a scan rate of only 20 mV s⁻¹, which is an indication of slow electron transport and transfer processes [15]. On the other side, the scan rate dependency of the peak current shows the linear behaviour expected for surface bound electro-active material, where the scan rate dependency is not influenced by its diffusion to and from the electrode (see Fig. 7, inset).⁵

Two possible mechanisms for the polymerisation can be taken into account and are pictured in Scheme 3.

Thiophenes are known to dimerize via a radical cation mechanism through the 2- and 5-positions (Scheme 3A) [22], which eventually leads for complexes with multiple thiophene substituents on the ligands to polythiophene type polymers with metal complexes in the backbone. However, in the present case the positive

⁵ From the area under the redox signals, the charge and therefore the absolute number of complex entities deposited on the electrode and incorporated into the polymer network can be calculated. For example, the evaluation of the redox peaks shown in Fig. 7 gives a total charge of 3.5 × 10⁻⁵ C, which corresponds to 3.6 × 10⁻¹⁰ mol of complex **5** deposited on the electrode. Taking into account the surface of the electrode and that a monolayer of these complexes includes about 7.7 × 10⁻¹¹ mol cm⁻² (J. Am. Chem. Soc. 116 (1994) 5444), the thickness of the polymer is equivalent to 66 monolayers and therefore the thickness of the polymer layer is in the order of 50–100 nm after 16 deposition cycles, assuming an average Ru–Ru distance of 15–20 Å.



Scheme 3.

charge can delocalize towards the olefinic double bond, which will eventually dimerize (Scheme 3B) and therefore offers an alternative pathway for reaction of the oxidized species [22–26].

Absorption spectra of the polymers on FTO-glass have been recorded, and the influence of the polymerisation method is clearly seen, as exemplified for **6** (see Fig. 8) and listed in Table 3.

The blue shift of the MLCT, which we find for all oxidatively produced polymers, points towards a loss of conjugation as it is depicted in Fig. 8. The disappearance of the LC-transition for the substituted ligand at 360 nm confirms the loss of conjugation in the ligand structure (see Fig. 8).

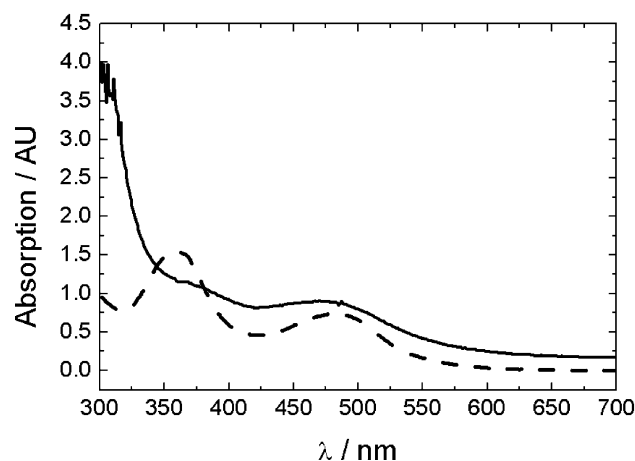


Fig. 8. Absorption spectra of polymer films of **5**, deposited on glass with a conducting layer of fluorine doped tin oxide (FTO) (solid line), and of the monomer **5** in solution (dashed line).

4. Conclusions

We have reported the synthesis, characterisation and polymerisation behaviour of four thiophene substituted ruthenium complexes. The polymerisation behaviour of the complexes at positive potentials showed the behaviour of a redox active film. No polymerisation was observed at negative potentials showing the low reactivity of the vinyl functionality in these complexes. The shift of the MLCT band of the absorption spectra towards shorter wavelengths in combination with an oxidation potential at less positive potentials implied a loss of conjugation within the ligands **3** and **4** due to a radical polymerisation through the vinyl functionality after delocalisation instead of the expected thiophene–thiophene coupling. Nevertheless, an interesting feature for an application in the NSC is the broader absorption spectrum of the dye compared to a ruthenium *tris*-bipyridyl complex. Also, the introduction of a thiophene-group makes this type of dye a possible base to form a solid-state solar cell by polymerisation. These compounds, used as a model, lay the ground for the development of new dyes possessing broader absorption properties and better water tolerance for solar cell application.

Acknowledgements

The authors thank the University of Uppsala and the Ångström Solar Center for support. E.F. acknowledges the European Community for the financial support (Marie-Curie Fellowship contract no. MCFI-2001-01264).

References

- [1] C.J. Brabec, N.S. Sariciftci, J.C. Hummelen, *Adv. Funct. Mater.* 11 (2001) 15.
- [2] A. Hagfeldt, M. Grätzel, *Acc. Chem. Res.* 33 (2000) 269.
- [3] V. Aranyos, J. Hjelm, A. Hagfeldt, H. Grennberg, *J. Chem. Soc. Dalton Trans.* (2001) 1319.
- [4] B.P. Sullivan, D.J. Salmon, T.J. Meyer, *Inorg. Chem.* 17 (1978) 3334.
- [5] T.A. Heimer, S.T. D'Arcangelis, F. Farzad, J.M. Stipkala, *Inorg. Chem.* 35 (1996) 5319.
- [6] A. Juris, V. Balzani, F. Barigilletti, S. Campagna, P. Belsler, A. von Zelewsky, *Coord. Chem. Rev.* 84 (1988) 85.
- [7] V. Skarda, M.J. Cook, A.P. Lewis, G.S.G. McAuli, A.J. Thomson, D.J. Robbins, *J. Chem. Soc., Perkin Trans. 2* (1984) 1293.
- [8] P.A. Mabrouk, M.S. Wrighton, *Inorg. Chem.* 25 (1986) 526.
- [9] J. Hjelm, E.C. Constable, E. Figgemeier, A. Hagfeldt, R. Handel, C.E. Housecroft, E. Mukhtar, E. Schofield, *Chem. Commun.* (2002) 284.
- [10] T.M. Pappenfus, K.R. Mann, *Inorg. Chem.* 40 (2001) 6301.
- [11] P. Hapiot, L. Gaillon, P. Audebert, J.J.E. Moreau, J.-P. Lère-Porte, M. Wong Chi Man, *Synth. Met.* 72 (1995) 129.

- [12] H Lund, in: H Lund, M.M. Baizer (Eds.), *Organic Electrochemistry*, 3rd ed., Marcel Dekker, New York, 1991, p. 301.
- [13] A. Juris, V. Balzani, F. Barigelletti, S. Campagna, P. Belser, A. von Zelewsky, *Coord. Chem. Rev.* 84 (1988) 85.
- [14] B.J. MacLean, P.G. Pickup, *J. Chem. Soc. Chem. Commun.* (1999) 2471.
- [15] M.O. Wolf, *Adv. Mater.* 13 (2001) 545.
- [16] A.J. Bard, L.R. Faulkner, *Electrochemical Methods: Fundamentals and Applications*, Wiley, New York, 1980.
- [17] R.C. Leidner, B.P. Sullivan, R.A. Reed, B.A. White, M.T. Crimmins, R.W. Murray, T.J. Meyer, *Inorg. Chem.* 26 (1987) 882.
- [18] P.D. Beer, O. Kocian, R.J. Mortimer, C. Ridgeway, *J. Chem. Soc. Faraday Trans.* 89 (1993) 333.
- [19] H. Segawa, F.P. Wu, N. Nakayama, H. Maruyama, S. Nagisaka, N. Higuchi, M. Fujitsuka, T. Shimidzu, *Synth. Met.* 71 (1995) 2151.
- [20] T. Shimidzu, H. Segawa, F. Wu, N. Nakayama, J. Photochem. Photobiol. A: Chem. 92 (1995) 121.
- [21] R.P. Kingsborough, T.M. Swager, *J. Mater. Chem.* 9 (1999) 2123.
- [22] J. Roncali, *Chem. Rev.* 92 (1992) 711.
- [23] V. Ruiz, A. Colina, A. Heras, J. Lopez-Palacios, R. Seeber, *Helv. Chim. Acta* 84 (2001) 3628.
- [24] Refs. [29] and [30] from previous reference: J. Heinze, P. Tschuncky, A. Smie, *J. Solid State Electrochem.* 2 (1998) 102.
- [25] Refs. [29] and [30] from previous reference: J.R. Lenhard, R.L. Parton, *J. Am. Chem. Soc.* 109 (1987) 5808.
- [26] M. Pagels, J. Heinze, B. Geschke, V. Rang, *Electrochim. Acta* 46 (2001) 3943, Citation: 'Recent studies of the oxidation of radical ions containing olefinic double bonds have shown that such radicalic species dimerises at one of the olefinic carbon atoms, forming dimers. The dimerisation process may be reversible.'